Chapter 33

Beta Rhythms

Oscillations at frequencies of approximately 12–30 Hz — roughly half the gamma frequency — are called *beta oscillations* or *beta rhythms* in neuroscience. Many experimental studies have linked beta oscillations to motor function. They are, in particular, more pronounced during holding periods, and attenuated during voluntary movement. Engel and Fries [44] have hypothesized that more generally, beta oscillations may signal the expectation or intent of maintaining a sensorimotor or cognitive *status quo*. (The *sensorimotor* areas of the brain are those that combine sensory and motor functions.) This fits with the observation that in patients suffering from Parkinson's disease and the associated slowed movement (*bradykinesia*), power and coherence of beta oscillations in the *basal ganglia* are abnormally high, and are attenuated by *levodopa*, a drug commonly used to treat Parkinson's disease [20].

Many mechanisms that can produce beta oscillations have been proposed, and it is thought that beta-band oscillations in different parts of the brain originate in different ways. Here we study just a few of the many possible mechanisms.

33.1 PING-Like Beta Rhythms

The interaction of E- and I-cells, as in PING, can produce oscillations at frequencies below the gamma range. We have already mentioned reference [175] as an example. In [175], oscillations in a model network at frequencies around 10 Hz arise from the interaction of excitatory and inhibitory cell populations. The inhibitory synapses in [175] are $GABA_B$ receptor-mediated, and therefore much slower than $GABA_A$ receptor-mediated ones.

A PING rhythm can in principle be slowed down from gamma frequency to beta frequency in several ways. For instance, we can (1) make inhibition

Electronic supplementary material: The online version of this chapter (doi: 10.1007/978-3-319-51171-9_33) contains supplementary material, which is available to authorized users.

C. Börgers, *An Introduction to Modeling Neuronal Dynamics*,
Texts in Applied Mathematics 66, DOI 10.1007/978-3-319-51171-9_33

longer-lasting, or (2) make inhibition stronger, or (3) lower the external drive to the E-cells. These three possibilities are illustrated by Figs. 33.1–33.3.

One must make the decay time constant of the I-to-E synapses very much longer (from 9 ms to 90 ms) to turn the gamma rhythm of Fig. 30.4 into the beta

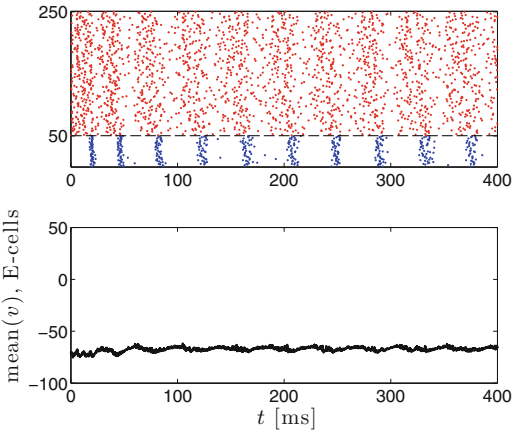

Figure 33.1. *Spike rastergram of an E-I network (top), and mean membrane potential of the E-cells (bottom). All parameters as in Fig. 30.4, except the decay time constant of I-to-E synapses is 90 ms here, while it was 9 ms in Fig. 30.4. (The decay time constant of I-to-I synapses is still 9 ms, as in Fig. 30.4.) Note that the simulated time interval is twice longer than in Fig. 30.4.* [PINB_1]

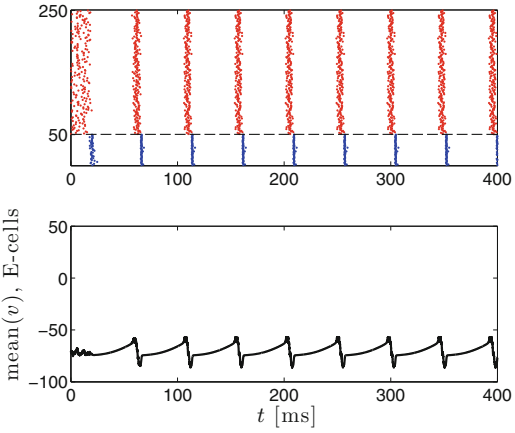

Figure 33.2. *Spike rastergram of an E-I network (top), and mean membrane potential of the E-cells (bottom). All parameters as in Fig. 30.4, except* $\hat{g}_{IE} = 10$ *here, while* $\hat{g}_{IE} = 0.25$ *in Fig. 30.4.* [PINB_2]

rhythm of Fig. 33.1. Also notice that the synchrony of the E-cells is fairly poor in Fig. 33.1. This is an effect of heterogeneity in external drives to the E-cells, and

heterogeneity in the number of inhibitory synaptic inputs per E-cell. The same level of heterogeneity has little effect in Fig. 33.2 (compare exercise 1). However, to turn the gamma rhythm of Fig. 30.4 into the beta rhythm of Fig. 33.2, one must strengthen I-to-E inhibition by a very large factor.

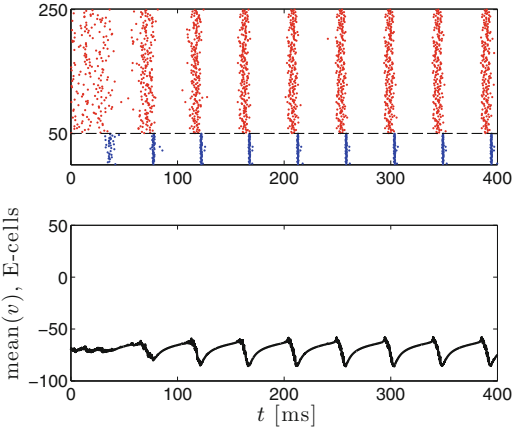

Figure 33.3. *Spike rastergram of an E-I network (top), and mean membrane potential of the E-cells (bottom). All parameters as in Fig. 30.4, except* $\overline{I}_E = 0.4$ *here, while* $\overline{I}_E = 1.4$ *in Fig. 30.4.* [PINB_3]

33.2 A Period-Skipping Beta Rhythm, and Cell Assemblies

In this section we describe a model introduced in [181], and simplified and studied in greater detail in [122]. The model explains experimental results presented in [181] and [122]. In these experiments, tetanic stimulation of a hippocampal slice generates a gamma oscillation, which after less than a second slows down and transitions into a beta oscillation.

From a more general point of view, these studies are about *cell assemblies*. The concept of a cell assembly was proposed in 1949 by the neuropsychologist Donald Hebb [73], and has been greatly influential in neuroscience. Hebb suggested that the brain represents information in the form of ensembles of neurons, which he called cell assemblies, firing together, with the information encoded in membership in the assembly.

Hebb's ideas about cell assemblies are closely linked to his hypotheses about *plasticity*, i.e., the modification of synaptic strengths as a result of experience, or learning. He suggested that if neuron A participates in making neuron B fire, then the excitatory synaptic connection from A to B will be strengthened [73]. This is often summarized by saying: "Neurons that fire together wire together." The slogan is memorable, but does not precisely reflect Hebb's hypothesis, as "together" suggests symmetry between A and B, whereas in Hebb's hypothesis, A and B clearly do not play the same role.

For an extension of Hebb's idea, referred to as *spike timing-dependent plasticity (STDP)*, experimental evidence was presented in [68]: The connection from A to B (pyramidal cells in layer V of rat neocortex) was shown to be strengthened when A fires just before B (*Hebbian learning*), and weakened when B fires just before A (*anti-Hebbian learning*). We will study a mathematical model of STDP in the last two chapters of this book.

For now, we return to [181] and [122]. The firing during the gamma oscillation activates an AHP current in the participating pyramidal cells [181], modeled as an M-current in [122]. This is one central ingredient for explaining the slow-down. It is, however, not the only ingredient. The introduction of an adaptation current by itself would simply generate a *clustered* gamma oscillation, i.e., it would lead to a reduction in the mean firing frequency of individual pyramidal cells, without bringing the population frequency into the beta range; see Section 32.2, and also Fig. 33.4.

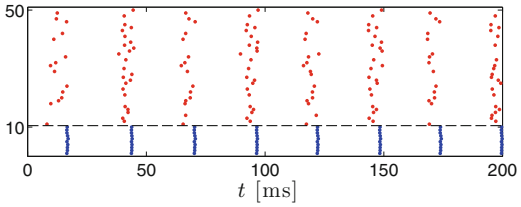

Figure 33.4. *Clustered PING rhythm similar to that in Fig. 32.6. The strength of the M-current is chosen deliberately here to create two clusters:* $\overline{g}_{\mathrm{M}} = 0.5$. *To make the details of the clustering easier to see, the number of neurons in the network is reduced:* $N_E = 40$, $N_I = 10$. *To obtain a network comparable to the larger one, the reduction in* N_E *and* N_I *must be accompanied by an increase in the connection probabilities* p_{EI}, p_{IE}, p_{II} *(see Section 30.3). Since sparseness and randomness of connectivity is not the main focus here, we simply use all-to-all connectivity. All other parameters are as in Fig. 32.6. The population frequency is slightly below 40 Hz.* [M_CURRENT_PING_4]

The second central ingredient in the model of [181] and [122] is plasticity. The gamma oscillation was shown in [181] to lead to a strengthening of excitatory synaptic connections among the pyramidal cells participating in the oscillation. The effect is that pyramidal cells that participate in the gamma oscillation don't cluster; they (approximately) synchronize during the later phase of the experiment; see Fig. 33.5. Note that the transition from Fig. 33.4 to Fig. 33.5 illustrates that recurrent excitation can *lower* the network frequency.

The E-to-E connectivity introduced here is symmetric: The connection from B to A is strengthened just as much as the connection from A to B. As pointed out earlier, this is not quite in line with the original Hebbian hypothesis, and certainly not with STDP as described in [68], but it is in line with yet another variation on the Hebbian hypothesis, formulated, for instance, in [32]: (a) Temporal correlation of pre- and post-synaptic activity will lead to synaptic strengthening, and (b) lack of correlation will lead to synaptic weakening.

In both the experiments and the model of [181] and [122], some E-cells participated in the gamma oscillation, while others did not. Following [122], we call the two groups the E_P-cells andthe E_S-cells (with P standing for *participating*, and S for

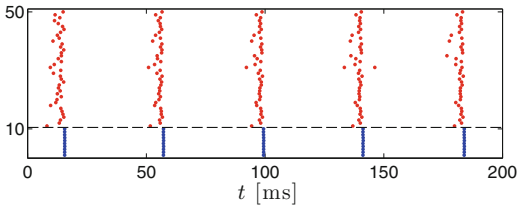

Figure 33.5. *Effect of introducing E-E connections ($\hat{g}_{EE} = 0.35$) in Fig. 33.4. There is now a beta rhythm with a frequency slightly under 25 Hz.* [M_CURRENT_PING_5]

suppressed). Experimentally, the separation into E_P- and E_S-cells was accomplished by treating some of the pyramidal cells with potassium-free artificial cerebrospinal fluid (ACSF), which lowers their excitability. In the model, different E-cells received different external drives. This can result in sharp *thresholding:* The most strongly driven E-cells participate on each cycle of the gamma oscillation, while (most of) the others do not participate at all; see Chapter 37.

The division of the E-cells into E_P- and E_S-cells makes the plasticity of the E-to-E connections selective: Only connections among E_P-cells are strengthened (or, in our model, created). Figure 33.6 shows what happens when in Fig. 33.5, only half the E-cells, the ones with neuronal indices 31 through 50, are connected synaptically.

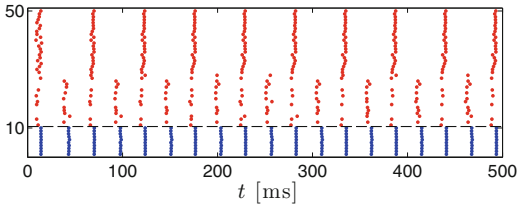

Figure 33.6. *Effect of introducing E-to-E connections only among cells 31 through 50 (half of all E-cells) in Fig. 33.4. There is a population gamma rhythm with two clusters. Those E-cells that are synaptically connected all belong to the same cluster, and therefore fire at half the gamma frequency, slightly below 20 Hz here.* [M_CURRENT_PING_6]

In [122], it was demonstrated, both experimentally and in the simulations, that (nearly) all E_S-cells fired on precisely those gamma cycles on which the E_P-cells did not fire. In other words, the two E-cell clusters were the E_P-cells and the E_S-cells. This *temporal separation* of E_P- and E_S-cells is not seen in Fig. 33.6, but can be reproduced in simulations when one includes other plastic changes likely

caused by the gamma oscillation. In [122], it was assumed that the E_S-to-I synapses are weakened during the gamma oscillation, when the E_S-cells are silent and the I-cells are active. Indeed, if we halve the strength of the E_S-to-I synapses in Fig. 33.6, fairly clean temporal separation of E_P-cells and E_S-cells results; see Fig. 33.7.

It is easy to see why weakening the E_S-to-I synapses will tend to promote temporal separation of E_P- and E_S-cells. Let us call the gamma cycles on which the E_P-cells fire the *on-beats*, and the gamma cycles on which they don't fire the *off-beats.* Weakening the E_S-to-I synapses causes the I-cell spike volleys on the off-beats to occur slightly later, and thereby allows more E_S-cells to fire on the off-beats. This falls short of explaining why the separation should become as clean as in Fig. 33.7, but in fact it is *not* always as clean; see exercise 2.

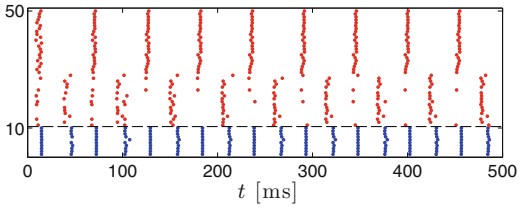

Figure 33.7. *Like Fig. 33.6, with the strengths of the synapses from E-cells 11 through 30 (the E_S-cells) cut in half.* [M_CURRENT_PING_7]

The reasoning of the preceding paragraph suggests another way of separating E_P- and E_S-cells into two nearly disjoint clusters: We can make the on-beats occur slightly earlier, for instance, by slightly raising external drive to the E_P-cells (but not to the E_S-cells). The E_P-cells participated in the gamma oscillation because they were more strongly driven, or perhaps because they were intrinsically more easily excitable, than the others. So greater external drive to the E_P-cells during the beta oscillation could be seen as a model of greater intrinsic excitability. Alternatively, the increased drive to the E_P-cells might also be thought of as reflecting slow recurrent excitation among the E_P-cells. Figure 33.8 shows that raising the drive to the E_P-cells can lead to the temporal separation of E_P- and E_S-cells even without altering the E_S-to-I synapses. The increased drive makes it easier for the E_P-cells to silence the E_S-cells on the on-beats.

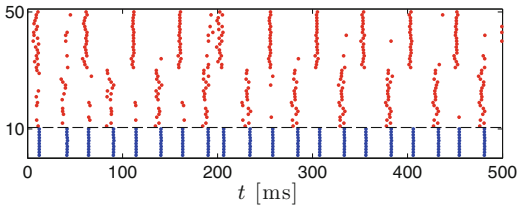

Figure 33.8. *Like Fig. 33.6, with the external drive to the E_P-cells (but not the E_S-cells) raised by 20%.* [M_CURRENT_PING_8]

We think of the E_P-cells as forming a Hebbian cell assembly. From this point of view, what is interesting about Figs. 33.7 and 33.8 is that plastic changes help the cell assembly, which started out firing at gamma frequency, survive the gamma-beta transition caused by the rising M-current.

33.3 A Non-synaptic Beta Rhythm

In [130], a beta rhythm in layer V of rat neocortical slices was examined experimentally and via computer simulations. An interesting feature of this rhythm is that it survives disruption of AMPA- and $GABA_A$ receptor-mediated synaptic transmission. It does depend on gap junctions and M-currents.

The model in [130] is quite complex. Most of the model neurons, the ones that are primarily responsible for generating the rhythm, represent *intrinsically bursting* (IB) cells, a class of pyramidal cells in neocortex. (The RTM model, by contrast, represents *regular spiking* (RS) pyramidal cells.) The neuronal models have many compartments, and the gap junctions are assumed axo-axonal. The drive that gives rise to the rhythm is stochastic.

We will not re-implement this complex model here, but merely show in Fig. 33.9 that the combination of M-currents and gap junctions can, in a network of RTM neurons, generate a beta frequency oscillation. We model gap junctions as described in Chapter 21, with

$$g_{\text{gap},ij} = \begin{cases} \hat{g}_{\text{gap}} / \left(p_{\text{gap}}(N-1)\right) & \text{with probability } p_{\text{gap}}, \\ 0 & \text{with probability } 1 - p_{\text{gap}}, \end{cases}$$

where N denotes the number of neurons in the network; $N = 200$ in Fig. 33.9. The cells in Fig. 33.9 fire in (loosely defined) clusters; see exercise 4.

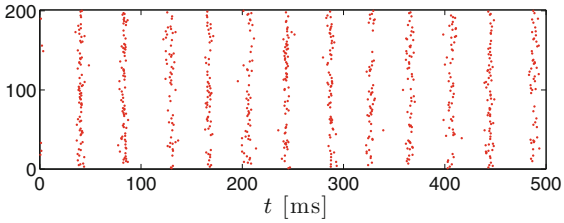

Figure 33.9. *A network of 200 RTM neurons, with M-currents ($\overline{g}_{\text{M}} = 1$) and gap junctions ($p_{\text{gap}} = 0.1$, $\hat{g}_{\text{gap}} = 0.2$) but no synaptic connections. Other parameters here are $\overline{I}_E = 3$ and $\sigma_E = 0.05$.* [M_CURRENT_BETA_WITH_GJ]

Exercises

33.1. (∗) A PING rhythm can be slowed down to beta frequency by increasing τ_I, the decay time constant of inhibition (Fig. 33.1), or by raising $\hat{g}_{IE}$, the parameter determining the strength of I-to-E synapses (Fig. 33.2). Comparison

of the two figures shows that the effects of drive heterogeneity become large when τ_I is raised, not when $\hat{g}_{IE}$ is raised. We won't give a rigorous explanation of this observation. However, plot $0.25e^{-t/90}$ and $10e^{-t/9}$ as functions of $t \in [0, 50]$ in a single figure, and explain why what you see yields at least a heuristic explanation.

33.2. (∗) The nearly strict temporal separation of E_P- and E_S-cells seen in Fig. 33.7 is not a completely robust effect. To see this, halve the strength of the E_S-to-I synapses in Fig. 33.7 once more. You will see that the temporal separation of E_P- and E_S-cells becomes a bit less clean.

33.3. (∗) What happens if in Fig. 33.6, you halve the strengths of the E_S-to-I synapses *and* raise the drive to the E_P-cells by 20%?

33.4. (∗) Demonstrate numerically that the cells in Fig. 33.9 fire in (loosely defined) clusters.